GEOPHYSICS, VOL. 58, NO. 6 (JUNE 1993); P. 797-809, 12 FIGS.

A finite-difference, time-domain solution for three-dimensional electromagnetic modeling

Tsili Wang* and Gerald W. Hohmann†

ABSTRACT

We have developed a finite-difference solution for three-dimensional (3-D) transient electromagnetic problems. The solution steps Maxwell's equations in time using a staggered-grid technique. The time-stepping uses a modified version of the Du Fort-Frankel method which is explicit and always stable. Both conductivity and magnetic permeability can be functions of space, and the model geometry can be arbitrarily complicated. The solution provides both electric and magnetic field responses throughout the earth. Because it solves the coupled, first-order Maxwell's equations, the solution avoids approximating spatial derivatives of physical properties, and thus overcomes many related numerical difficulties. Moreover, since the divergence-free condition for the magnetic field is incorporated explicitly, the solution provides accurate results for the magnetic field at late times.

An inhomogeneous Dirichlet boundary condition is imposed at the surface of the earth, while a homogeneous Dirichlet condition is employed along the subsurface boundaries. Numerical dispersion is alleviated by using an adaptive algorithm that uses a fourth-order difference method at early times and a second-order method at other times. Numerical checks against analytical, integral-equation, and spectral differential-difference solutions show that the solution provides accurate results.

Execution time for a typical model is about 3.5 hours on an IBM 3090/600S computer for computing the field to 10 ms. That model contains 100 x 100 x 50 grid points representing about three million unknowns and possesses one vertical plane of symmetry, with the smallest grid spacing at 10 m and the highest resistivity at 100 $\Omega \cdot$ m. The execution time indicates that the solution is computer intensive, but it is valuable in providing much-needed insight about TEM responses in complicated 3-D situations.

INTRODUCTION

Solving three-dimensional (3-D) transient electromagnetic (TEM) problems is important in understanding the physics of observed responses, and in providing insight for data interpretation. This paper describes a finite-difference solution to a general 3-D TEM problem. The solution, which is based on time-stepping Maxwell's equations, computes both electric and magnetic responses of arbitrarily complicated earth structures.

For more than a decade, finite-difference methods have been used, for their simplicity and flexibility, to solve two-dimensional (2-D) time-domain problems (Goldman and Stoyer, 1983; Oristaglio and Hohmann, 1984; among others). The development of a satisfactory finite-difference solution to 3-D time-domain problems has been slow, because of numerical difficulties as well as computer limitations. For example, Adhidjaja and Hohmann (1989) solved the second-order equations obtained by eliminating the electric field from Maxwell's equations, and found serious difficulty in accurately evaluating the derivatives of the physical properties. Solving the second-order equations may also encounter the problem of simulating discontinuous fields.

These problems can be overcome by solving the coupled, first-order Maxwell's equations using a staggered-grid scheme (Yee, 1966). Successful applications of the Yee scheme include EM wave scattering problems (e.g., Taflove and Brodwin, 1975; Holland et al., 1980; Taflove, 1980; Greenfield and Wu, 1991; Moghaddam et al., 1991), seismic modeling (e.g., Virieux, 1984, 1986), and magnetotelluric modeling and inversion (Madden and Mackie, 1989). Bergeal (1982) pioneered the application of the method to a TEM

Presented at the 61st Annual International Meeting, Society of Exploration Geophysicists. Manuscript received by the Editor February 17, 1992; revised manuscript received August 3, 1992.
*University of Utah, Dept. of Geology and Geophysics, Salt Lake City, UT 84112.
†Deceased.

problem in geophysics. Unfortunately, he was not able to step the field in large enough time steps because he tried to simulate weak displacement currents. Using a staggered grid, Druskin and Knizhnerman (1988) developed a spectral differential-difference solution to a 3-D transient problem, in which the original partial differential equations are reduced to ordinary differential equations. Luo (1989) proposed a time-domain, finite-difference scheme for solving 2-D and 2.5-D quasi-static Maxwell's equations. Using a divergence-free condition for the magnetic field, he solved for only two components of the magnetic field using variable time steps.

In this paper, we use Yee's (1966) staggered-grid scheme combined with a modified version of the Du Fort-Frankel (1953) scheme to discretize the quasi-static Maxwell's equations. In the following sections, we will (1) illustrate our finite-difference, time-domain (FDTD) formulation, (2) describe the boundary conditions and their numerical implementation and initialization of the time-stepping, and (3) present numerical checks of the solution against other solutions, including analytical, integral-equation, and spectral differential-difference methods, for a number of models.

THEORY

Governing equations

Under the quasi-static approximation, the TEM fields in linear, isotropic, and source-free media are described by Maxwell's equations (Hohmann, 1988)

$$-\frac{\partial \mathbf{b}(\mathbf{r}, t)}{\partial t} = \nabla \times \mathbf{e}(\mathbf{r}, t), \tag{1}$$

$$\mathbf{j}(\mathbf{r}, t) = \nabla \times \mathbf{h}(\mathbf{r}, t), \tag{2}$$

$$\nabla \cdot \mathbf{b}(\mathbf{r}, t) = 0, \tag{3}$$

$$\nabla \cdot \mathbf{j}(\mathbf{r}, t) = 0, \tag{4}$$

with

$$\mathbf{b}(\mathbf{r}, t) = \mu(\mathbf{r})\mathbf{h}(\mathbf{r}, t), \tag{5}$$

$$\mathbf{j}(\mathbf{r}, t) = \sigma(\mathbf{r})\mathbf{e}(\mathbf{r}, t), \tag{6}$$

where b(r, *t*) , h(r, *t*) , and e(r, *t*) are the magnetic induction, magnetic field, and electric field, respectively; a(r) and p(r) are the conductivity and magnetic permeability of the earth; and j(r, *t*) is the conduction current density.

Equations (1)-(4) are not completely independent of each other (Chew, 1990). In fact, taking the divergence of equation (1) plus an initial condition on V l b leads to equation (3) and taking the divergence of equation (2) leads to equation (4). In a numerical solution, however, equation (3) has to be incorporated explicitly. Otherwise, results are erroneous at late times, which has been confirmed by our numerical experience. To illustrate, consider the dc limit. In this case, equation (1) reduces to

$$\nabla \times \mathbf{e}(\mathbf{r}, t) = 0. \tag{7}$$

Now equation (3) is not derivable from equation (7). As a result, the magnetic field is non-unique, since an arbitrary gradient field can be added to h without violating equation (2). Thus, in the static limit equation (3) is needed.

In the presence of numeric noise, a transient magnetic field may also experience the instability at certain delay times, depending upon the time variation of the field. At early times, the transient field has sharp variations in time and the electric and magnetic fields strongly interact with each other; therefore the problem is nearly undetectable. As time progresses, the field is smoothed out and approaches the dc limit. The problem then becomes increasingly severe. The later the time, the larger the arbitrary gradient field can be. Best et al. (1985) discussed the problem in the frequency domain. They found that the low-frequency magnetic response can be erroneous if equation (3) is ignored. In the following, we will discuss the incorporation of equation (3) with equations (1) and (2).

Equation (3) implies that only two out of the three components of b are independent of each other; any one of them can be computed from the remaining two (Chew, 1990). This suggests a way of incorporating the equation (M. L. Oristaglio, 1991, pers. comm.): computing two components of b from equation (1) and the other component from equation (3), that is,

$$-\frac{\partial b_x}{\partial t} = \frac{de,}{\partial y} - \frac{\partial e_y}{\partial z}, \tag{8}$$

$$-\frac{\partial b_y}{\partial t} = \frac{\partial e_x}{\partial z} - \frac{\partial e_z}{\partial x}, \tag{9}$$

$$\frac{\partial b_z}{\partial z} = -\frac{\partial b_x}{\partial x} - \frac{\partial b_y}{\partial y}. \tag{10}$$

Boundary conditions

Maxwell's equations imply the following continuity conditions across boundaries in material properties:

(1) continuity of tangential electric and magnetic fields,
(2) continuity of normal components of total current and magnetic flux.

These conditions are used in the following section to define continuous fields on a staggered grid.

Also, for the solution to be unique, equations (2), (5), (6), and (8) to (10) are supplemented with domain boundary conditions. The following conditions are sufficient to give a unique solution: the tangential components of either e or b defined on the boundary, or the tangential components of e defined on part of the boundary and the tangential components of b on the remainder of the boundary. As boundary conditions in this study, we use the tangential e on the subsurface boundary and the tangential b on the surface of the earth. These conditions can be readily included in our numerical solution.

If the model and the source possess one plane of symmetry, natural boundary conditions can be applied on the symmetry plane. Then it is only necessary to discretize and compute half of the model.

Sources

In regions containing sources, equations (5) and (6) must be modified to

$$\mathbf{b}(\mathbf{r}, t) = \mu(\mathbf{r})\mathbf{h}(\mathbf{r}, t) + \mu_0 \mathbf{m}_p(\mathbf{r}, t),$$

$$\mathbf{j}(\mathbf{r}, t) = \sigma(\mathbf{r})\mathbf{e}(\mathbf{r}, t) + \mathbf{j}_p(\mathbf{r}, t),$$

where $\mathbf{m}_p(\mathbf{r}, t)$ and $\mathbf{j}_p(\mathbf{r}, t)$ are the impressed electric and magnetic current densities, and μ_0 is the magnetic permeability of free space. To avoid source singularities, we replace the source terms with initial conditions for e and b at $t = t_0 > 0$. (All sources are assumed to be shut off at $t = 0$.) Transforming to an initial boundary value problem from the original boundary value problem was discussed in Stakgold (1968) and has been applied by Oristaglio and Hohmann (1984) to a 2-D problem. Choosing an appropriate t_o, as discussed later, can provide a smooth initial condition so that the field is adequately sampled and numerical dispersion is reduced to a minimum.

NUMERICAL SOLUTION

In this section a finite-difference, time-stepping solution is derived for the system of equations (2), (5), (6), and (8) to (10). The solution is built of four distinct but integrated parts: (1) model discretization and time-stepping, (2) difference approximations to the spatial and time derivatives, (3) numerical implementation of the boundary conditions, and (4) initialization of the time stepping.

Model discretization and time stepping

The earth model is discretized into a number of prisms as shown in Figure 1. A Cartesian coordinate system is defined with its z-axis positive downward. The origin of the coordinates is placed at the upper, far left corner of the grid. The indices i, j, and k are used to number the grid point locations in the x, y, and z directions, respectively. Conductivity and magnetic permeability are assumed to be blockwise constant. The grid spacing is smallest near the source (represented by the thick arrow in the figure) and is enlarged gradually away from the source. Use of the graded grid is feasible because a diffusive EM field has relatively sharp variations near the source and is gradually smoothed away from the source (Oristaglio and Hohmann, 1984). To ensure adequate sampling of the field, we enlarge the grid spacing by an empirically determined factor of no larger than 2 from one block to the next. When the dimension of the source is small or the physical property contrasts of the model are large, the factor should be reduced.

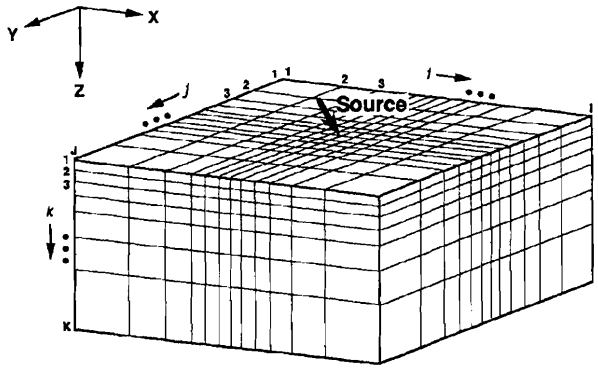

FIG. 1. Discretization of a 3-D earth model. The thick arrow stands for the source. Grid spacing increases laterally and vertically away from the source.

A staggered grid (Yee, 1966) is used to define the electric and magnetic fields, as shown in Figure 2a. The electric field components are located at the center of the edges, while the magnetic field components are located at the center of the faces. An important consequence of the staggered grid is that, with proper placement of the blockwise conductivity and magnetic permeability distributions, all the fields are continuous.

The staggered grid is composed of two elementary loops: an electric loop and a magnetic loop (Nekut and Spies, 1989;

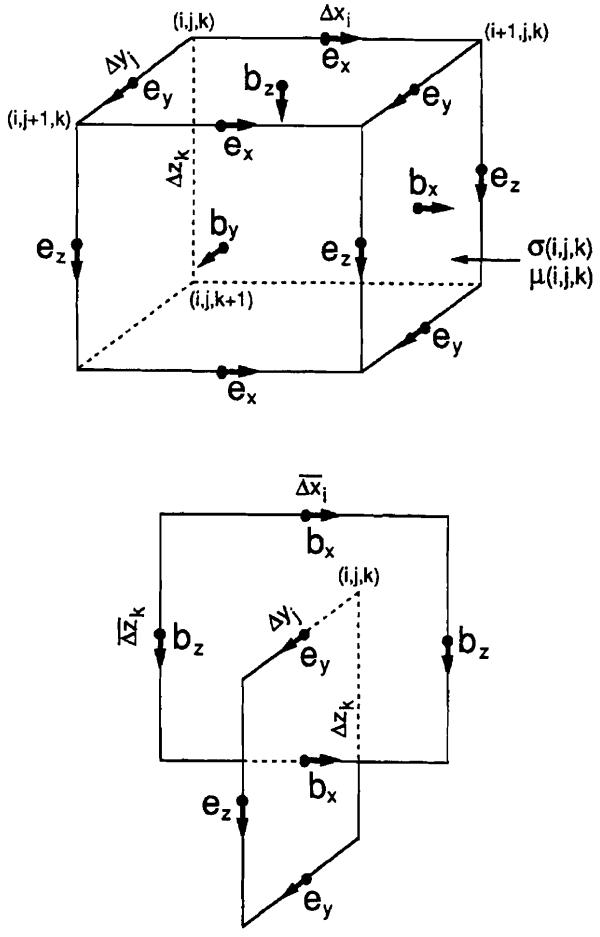

FIG. 2. (a) A staggered grid (after Yee, 1966). The electric field is sampled at the centers of the prism edges, and the magnetic field is sampled at the centers of the prism faces. (b) Interaction between an electric loop and a magnetic loop. The electric loop is formed by the four adjacent electric field components bounding a prism face. The magnetic loop is formed by the four adjacent magnetic field components, $\overline{\Delta x}_i = (\Delta x_{i-1} + \Delta x_i)/2$ and $\overline{\Delta z}_k = (\Delta z_{k-1} + \Delta z_k)/2$.

Visscher, 1989). The electric loop is formed by the four e components bounding the same face of a prism, while the magnetic loop is composed of the four adjacent b components. An example is shown in Figure 2b. The concept of the elementary loops is very useful in discretizing Maxwell's equations.

In this paper, we use a modified version of the Du Fort-Frankel method to time step equations (1) and (2). The Du Fort-Frankel (Du Fort and Frankel, 1953) method is explicit and unconditionally stable as applied to a diffusion equation (Birtwistle, 1968). Based on the method, Oristaglio and Hohmann (1984) presented a solution to a 2-D problem. Later, Adhidjaja and Hohmann (1989) applied it to a 3-D problem in which they attempted without success to solve the second-order differential equations for the magnetic field.

The essence of the Du Fort-Frankel method is the *implicit* introduction of a hyperbolic term into the parabolic equation. All that is needed is to keep the velocity of the fictitious wavefield slower than that simulated by the finite-difference scheme. To apply the Du Fort-Frankel method to the first-order system, we explicitly solve a wave-like equation obtained by modifying equation (2) to

$$\gamma \frac{\partial \mathbf{e}(\mathbf{r}, t)}{\partial t} + \sigma(\mathbf{r})\mathbf{e}(\mathbf{r}, t) = \nabla \times \mathbf{h}(\mathbf{r}, t), \tag{11}$$

where γ is a coefficient we shall define later. The first term on the left-hand side resembles a displacement current; it is, however, purely artificial (see also Chew, 1990). By appropriately defining γ, we can develop an explicit, always stable, time-stepping solution.

We use the indices, 0, 1, 2, . . . , n - 1, n, . . . to represent the time instants, $t_0, t_1, \ldots, t_{n-1}, t_n$, with $t_n = t_{n-1} + \Delta t_{n-1}$. Following Yee's (1966) time-staggering scheme, we define the electric field at integer time indices along the time axis, and the magnetic field at intermediate time indices. We carry out time-stepping in a leap-frog fashion; given e at $t \le t_n$ and b at $t \le t_n + \Delta t_n/2$, we extrapolate e to $t = t_{n+1}$ using equation (2); then with b at $t \le t_n + \Delta t_n/2$ and e at $t \le t_{n+1}$, we extrapolate b to $t = t_{n+1} + \Delta t_{n+1}/2$ using equation (1), and so on.

Finite-difference equations

For convenience, we rewrite equation (11) in component form

$$\gamma \frac{\partial e_x}{\partial t} + \sigma e_x = \frac{\partial h_z}{\partial y} - \frac{\partial h_y}{\partial z}, \tag{12}$$

$$\gamma \frac{\partial e_y}{\partial t} + \sigma e_y = \frac{\partial h_x}{\partial z} - \frac{\partial h_z}{\partial x}, \tag{13}$$

and

$$\gamma \frac{\partial e_z}{\partial t} + \sigma e_z = \frac{\partial h_y}{\partial x} - \frac{\partial h_x}{\partial y}. \tag{14}$$

We first discretize equations (8) and (13) as representatives of the time-stepping system. Then we discuss a difference approximation to equation (10), followed by numerical evaluation of equation (5) on a staggered grid. The notation $b_x^{n+1/2}(i, j + 1/2, k + 1/2)$ is used to represent the x-directed magnetic field at grid node $(i, j + 1/2, k + 1/2)$ and at time instant $t_n + \Delta t_n/2$. Similar notations are used for the other field components. Applying the integral form of equation (8)

$$-\int\int \frac{\partial b_x}{\partial t} = \oint (\mathbf{e} \times \mathbf{u}_x) \cdot d\mathbf{l},$$

where $\mathbf{u}_x$ is an x-directed unit vector and 1 is in the yz-plane to the electric loop in Figure 2b, and approximating $\partial b_x / \partial t$ at time level n using a central difference

$$\left(\frac{\partial b_x}{\partial t}\right)^n \approx \frac{b_x^{n+1/2} - b_x^{n-1/2}}{(\Delta t_{n-1} + \Delta t_n)/2},$$

we obtain

$$\begin{aligned} b_x^{n+1/2}&(i, j + 1/2, k + 1/2) \\ &= b_x^{n-1/2}(i, j + 1/2, k + 1/2) - \frac{\Delta t_{n-1} + \Delta t_{n+1}}{2} \\ &\times \left[\frac{e_z^n(i, j + 1, k + 1/2) - e_z^n(i, j, k + 1/2)}{\Delta y_j}\right. \\ &\left. - \frac{e_y^n(i, j + 1/2, k + 1) - e_y^n(i, j + 1/2, k)}{\Delta z_k}\right]. \end{aligned} \tag{15}$$

In deriving equation (15), we assume that b_x is constant across the entire electric loop area, and that e_y and e_z are constant along the y- and z- directed edges of the loop, respectively. A similar difference equation can be derived for equation (9).

Similarly, application of the integral form of equation (13) to the magnetic loop in Figure 2b, and approximation of $\partial e_y / \partial t$ at time level $n + 1/2$ by a central difference

$$\left(\frac{\partial e_y}{\partial t}\right)^{n+1/2} \approx \frac{e_y^{n+1} - e_y^n}{\Delta t_n},$$

and $e_y^{n+1/2}$ by the average of e_y^n and e_y^{n+1}

$$e_y^{n+1/2} \approx \frac{e_y^n + e_y^{n+1}}{2},$$

lead to the difference equation for extrapolating e_y

$$\begin{aligned} e_y^{n+1}&(i, j + 1/2, k) \\ &= \frac{2\gamma - \Delta t_n \sigma(i, j + 1/2, k)}{2\gamma + \Delta t_n \sigma(i, j + 1/2, k)} e_y^n(i, j + 1/2, k) \\ &\times \frac{2\Delta t_n}{2\gamma + \Delta t_n \sigma(i, j + 1/2, k)} \\ &\times \left[\frac{h_x^{n+1/2}(i, j + 1/2, k + 1/2) - h_x^{n+1/2}(i, j + 1/2, k - 1/2)}{\overline{\Delta z}_k}\right. \\ &\left. - \frac{h_z^{n+1/2}(i + 1/2, j + 1/2, k) - h_z^{n+1/2}(i - 1/2, j + 1/2, k)}{\overline{\Delta x}_i}\right], \end{aligned} \tag{16}$$

with

$$\overline{\Delta x}_i = \frac{\Delta x_{i-1} + \Delta x_i}{2},$$

$$\overline{\Delta z}_k = \frac{\Delta z_{k-1} + \Delta z_k}{2}.$$

In the above equation, $\sigma(i, j + 1/2, k)$ is the averaged conductivities of the four prisms connected by the magnetic loop

$$\sigma(i, j + 1/2, k) = \sum_{p=0}^{1} \sum_{q=0}^{1} \sigma(i - p, j, k - q) w(i - p, j, k - q),$$

where w is a weighting function evaluated as the ratio of the area of a particular prism cut by the magnetic loop to the total area of the loop. In deriving equation (16), we assume that e_y and its time derivative are constant across the entire magnetic loop area, and b_x and b_z are constant over the edges of the loop on which they reside. The difference equations for equations (12) and (14) can be obtained in the same way.

Approximation of equation (10) is straightforward. Note that the divergence of b can be readily approximated at the center of a prism using its components on the six faces of the prism. Thus we obtain

$$\frac{b_z^{n+1/2}(i + 1/2, j + 1/2, k + 1) - b_z^{n+1/2}(i + 1/2, j + 1/2, k)}{\Delta z_k} = -\frac{b_x^{n+1/2}(i + 1, j + 1/2, k + 1/2) - b_x^{n+1/2}(i, j + 1/2, k + 1/2)}{\Delta x_i} - \frac{b_y^{n+1/2}(i + 1/2, j + 1, k + 1/2) - b_y^{n+1/2}(i + 1/2, j, k + 1/2)}{\Delta y_j}.$$

Rearranging the above equation leads to

$$b_z^{n+1/2}(i + 1/2, j + 1/2, k) = b_z^{n+1/2}(i + 1/2, j + 1/2, k + 1) + \Delta z_k \left[\frac{b_x^{n+1/2}(i + 1, j + 1/2, k + 1/2) - b_x^{n+1/2}(i, j + 1/2, k + 1/2)}{\Delta x_i} + \frac{b_y^{n+1/2}(i + 1/2, j + 1, k + 1/2) - b_y^{n+1/2}(i + 1/2, j, k + 1/2)}{\Delta y_j} \right]. \quad (17)$$

To solve the above equation, we start from the bottom boundary of the grid where $b_z = 0$ and step b_z upward.

Finally, the magnetic field, **h**, here used as an intermediate variable, can be calculated from b using averaged magnetic permeabilities. For example,

$$h_x(i, j + 1/2, k + 1/2) = b_x(i, j + 1/2, k + 1/2)/\mu(i, j + 1/2, k + 1/2), \quad (18)$$

where

$$\mu(i, j + 1/2, k + 1/2) = \frac{\Delta x_{i-1}\, \mu(i - 1, j, k) + \Delta x_i\, \mu(i, j, k)}{\Delta x_{i-1} + \Delta x_i}.$$

The system of difference equations (15) to (17) have second-order accuracy in space and time. Each field variable is stored only at one time level.

Stability

The time-stepping system defined by equations (15) to (18) is explicit and always stable if

$$\gamma \geq \frac{3}{\mu_{min}} \left(\frac{\Delta t_n}{\Delta_{min}} \right)^2, \quad (19)$$

where Δ_{min} is the minimum grid spacing, and μ_{min} is the minimum value of the magnetic permeability. To see this, note that the phase velocity of the wave-like field defined by equations (1) and (11) can be written

$$v = \frac{1}{\sqrt{\mu\gamma}}.$$

Substituting γ from equation (19), we obtain

$$v \leq \frac{\Delta_{min}}{\sqrt{3}\Delta t_n} \sqrt{\frac{\mu_{min}}{\mu}} \leq \frac{\Delta_{min}}{\sqrt{3}\Delta t_n},$$

which is exactly the Courant-Friedrichs-Lewy condition (Mitchel and Griffiths, 1980) for a wave equation, except that the time step is now variable.

The artificial term in equation (11) acts as a displacement current. In fact, its magnitude can be much larger than the real displacement current in a nonpolarizable medium. For example, a time step of 1 μs, a minimum grid spacing of 10 m, and $\mu_{min} = \mu_0$ gives $\gamma \approx 2.4 \times 10^{-8}$, a value about 2700 times as large as the free-space permittivity. To prevent the fictitious displacement current from dominating the diffusive EM field, we must constrain the length of the time step. One can show that the field retains its diffusive nature if (Oristaglio and Hohmann, 1984 and Adhidjaja and Hohmann, 1989)

$$\Delta t \ll \left(\frac{\mu_{min}\sigma t}{6}\right)^{1/2} \Delta_{min}, \tag{20}$$

where σ can be taken as the minimum conductivity in the model. In practice, one can use a time step

$$\Delta t_{max} = \alpha\left(\frac{\mu_{min}\sigma t}{6}\right)^{1/2} \Delta_{min}, \tag{21}$$

where α ranges from 0.1 to 0.2, depending on the accuracy required. Further reduction of α is unnecessary because of limited improvements on the accuracy of the results. Note that the time step given in equation (21) can be gradually enlarged with increasing time.

Boundary conditions

To ensure a unique solution, we impose Dirichlet conditions on all the domain boundaries. For convenience, we specify a tangential electric field on the subsurface boundaries, and a tangential magnetic field on the surface of the earth.

Subsurface boundaries.-On the subsurface boundaries, we simply set the tangential electric field to zero. This homogeneous Dirichlet condition is a good approximation to the true radiation condition only if the boundaries are far enough away from the source at a given time. Generally speaking, a less conductive earth or a larger source requires a larger grid, while computation of the early-time response needs a smaller grid than does that of the late-time response. Thus, an optimal grid should be used with its size adjusted with time for certain models. For simplicity, however, we have used a fixed but model-dependent grid. The grid is expected to be large enough to give reliable results at the latest time specified. Its horizontal dimensions are roughly three to four times larger than the radius of the equivalent descending current filament (Nabighian, 1979) at the latest time due to a source on the surface. The vertical dimension of the grid is about three fourths of its horizontal dimensions.

Air-earth interface. - A simple upward-continuation boundary condition can be implemented at the surface of the earth (Oristaglio and Hohmann, 1984). Two advantages follow: first, the grid size can be reduced; and second, it is not necessary to time-step the EM field in free space, which would require very small time steps to keep the solution stable. To apply the upward-continuation condition to the staggered grid, we extend the grid by one grid level into the air, and then compute b_x and b_y at a level of half a grid spacing *above* the surface of the earth, using the b_z on the surface.

Under the quasi-static assumption, the magnetic flux in free space obeys the vector Laplacian equation (Grant and West, 1965, p. 470)

$$\nabla^2 \mathbf{b} = 0. \tag{22}$$

It is well known (cf, Nabighian, 1972, 1984; Macnae, 1984) that the horizontal components of b satisfying equation (22) can be derived from its vertical component on the same horizontal plane. From equation (22), one can derive the following wavenumber-domain equations

$$\mathfrak{B}_x(u, v, z = 0) = -\frac{iu}{\sqrt{u^2 + v^2}} \mathfrak{B}_z(u, v, z = 0), \tag{23}$$

and

$$\mathfrak{B}_y(u, v, z = 0) = -\frac{iv}{\sqrt{u^2 + v^2}} \mathfrak{B}_z(u, v, z = 0), \tag{24}$$

where $\mathfrak{B}_x$, $\mathfrak{B}_y$, and $\mathfrak{B}_z$ are the Fourier transforms of b_x, b_y, and b_z, respectively; u and v are the wavenumber domain variables corresponding to x and y, respectively. The 2-D Fourier transform is defined as

$$F(u, v) = \int_{-\infty}^{\infty}\int_{-\infty}^{\infty} f(x, y) \exp\left[-i(ux + vy)\right] dx\, dy.$$

$\mathfrak{B}_x$ and $\mathfrak{B}_y$ given in equations (23) and (24) can be upward continued to give their values in free-space (Grant and West, 1965, p. 216-220), i.e.,

$$\mathfrak{B}_x(u, v, z = -h) = \exp\left(-h\sqrt{u^2 + v^2}\right)\mathfrak{B}_x(u, v, z = 0), \tag{25}$$

and

$$\mathfrak{B}_y(u, v, z = -h) = \exp\left(-h\sqrt{u^2 + v^2}\right)\mathfrak{B}_y(u, v, z = 0). \tag{26}$$

Substituting equation (23) into (25) and equation (24) into (26) yield

$$\mathfrak{B}_x(u, v, z = -h) = -\frac{iu}{\sqrt{u^2 + v^2}} \exp\left(-h\sqrt{u^2 + v^2}\right)\mathfrak{B}_z(u, v, z = 0), \tag{27}$$

and

$$\mathfrak{B}_y(u, v, z = -h) = -\frac{iv}{\sqrt{u^2 + v^2}} \exp\left(-h\sqrt{u^2 + v^2}\right)\mathfrak{B}_z(u, v, z = 0). \tag{28}$$

Implementation of equations (27) and (28) is as follows. First, we interpolate, using a bicubic spline function (see also Adhidjaja and Hohmann, 1989), the nonuniform grid spanned by the discrete b_z values on the ground surface to a constant grid with grid spacing δ. Then we Fourier transform b_z into the wavenumber domain and multiply the results by the operating coefficients in the equations. Finally, we inverse Fourier transform the results into the space-domain.

The computer cost of the whole process is dominated by the forward and inverse Fourier transforms that are proportional to $N \log_2 N$, where N is the total number of data points in both x- and y- directions. At the beginning of time stepping, we take δ to be the same as the smallest grid spacing. We then increase δ, on a linear-square root plot, with time while keeping the overall sampling area fixed. This results in a reduction of N with time. Here, we have used the fact that the TEM field is smoothed gradually in space with time, and thus the sampling rate can be reduced accordingly.

Initial conditions

To initialize the time-stepping, we supply initial conditions for e at $t = t_0$ and for b at $t = t_o + \Delta t_0/2$, respectively, where $t_o > 0$ and Δt_0 is the initial time step. We assume that the top part of the earth is homogeneous (Oristaglio and Hohmann, 1984), and compute the field there using an analytical solution for a uniform half-space. The quality of the initial conditions is controlled by t_o. In principle, t_o should be small enough such that the assumption of a uniform half-space solution is valid. On the other hand, it should be large enough so that the field is adequately sampled. If t_o is too small, numerical grid dispersion may result from undersampling of the field. In some cases where the inhomogeneities are shallow or the field is required at very early time, one should use a higher-order differencing algorithm to suppress the numerical dispersion. In the next section, we shall discuss an adaptive algorithm that employs a fourth-order finite-difference scheme at early times and a second-order scheme at later times.

Based on a series of experiments in which the finite-difference, time-domain (FDTD) results were compared to the analytical solution for a horizontal magnetic dipole on the surface of a uniform half-space (Ward and Hohmann, 1988), we found that setting

$$t_0 = 1.13\mu_1\sigma_1\Delta_1^2,$$

is appropriate, where μ_1 and σ_1 are, respectively, the magnetic permeability and conductivity of the top layer, and Δ_1 is the grid spacing of the uppermost part of the grid. In the above equation, t_0 corresponds to the time when the equivalent current filament (Nabighian, 1979) of the magnetic dipole penetrates to a depth of $1.5\Delta_1$.

In this study, we incorporate the impulse responses of e and b as the initial conditions so that the algorithm computes the impulse response of b. To do that, we first compute the step response of e (San Filipo and Hohmann, 1985) down to about five grid levels in the earth, with the electric field one grid level above the surface computed using an equation similar to equation (25). Next, we compute the impulse b response using equation (1) which in turn is substituted into equation (2) to give the impulse e response.

NUMERICAL DISPERSION AND ADAPTIVE ALGORITHM

Numerical dispersion occurs whenever a finite grid is unable to simulate a high-frequency field. Consider a uniform grid with spacing A. To suppress the numerical dispersion to an acceptable level, the spatial sampling rate must honor (Alford et al., 1974 and Kelly et al., 1976)

$$\frac{\lambda_{min}}{\Delta} \geq N, \tag{29}$$

where λ_{min} is the minimum wavelength and N is the smallest number of grid points per wavelength. The value of N depends on the difference approximation scheme used. In general, a higher order algorithm has a better ability to suppress the numerical dispersion, and thus requires a lower sampling rate. For a second-order scheme, N should be no less than 10, while for a fourth-order scheme it should be no less than 5 (Alford et al., 1974).

Numerical dispersion also occurs in the finite-difference modeling of a diffusive EM field. Consider the transient field induced in a conductive earth by shutting off a steady source current. Shortly after the shut-off the field is dominated by high-frequencies and rapid spatial variations. As time progresses, the high frequencies are attenuated and the field becomes smoother in space. Therefore, numerical dispersion should occur more likely at early times.

In our adaptive algorithm, we use a fourth-order scheme at early times. The fourth-order scheme approximates the spatial derivatives using fourth-order differences; e.g.,

$$\begin{aligned} b_x^{n+1/2}&(i, j+1/2, k+1/2) \\ &= b_x^{n-1/2}(i, j+1/2, k+1/2) - \frac{\Delta t_{n-1} + \Delta t_{n+1}}{2} \\ &\quad \cdot \times \sum_{p=-1}^{2} [a_p e_z^n(i, j+p, k+1/2) \\ &\quad - b_p e_y^n(i, j+1/2, k+p)], \end{aligned} \tag{30}$$

$$\begin{aligned} e_y^{n+1}&(i, j+1/2, k) \\ &= \frac{2\gamma - \Delta t_n \sigma(i, j+1/2, k)}{2\gamma + \Delta t_n \sigma(i, j+1/2, k)} e_y^n(i, j+1/2, k) \\ &\quad + \frac{2\Delta t_n}{2\gamma + \Delta t_n \sigma(i, j+1/2, k)} \\ &\quad \times \sum_{p=-1}^{2} [c_p h_x^{n+1/2}(i, j+1/2, k+p-1/2) \\ &\quad - d_p h_z^{n+1/2}(i-p+1/2, j+1/2, k)], \end{aligned} \tag{31}$$

where a, b, c, and d are the sets of difference coefficients, an example of which is given in the Appendix. To keep time stepping of equations (30) and (31) always stable, we modify equation (19) to (see also Mufti, 1990, for a discussion of seismic wave modeling)

$$\gamma \geq \frac{4}{\mu_{min}} \left(\frac{\Delta t_n}{\Delta_{min}}\right)^2,$$

and accordingly reduce the maximum time step to

$$\Delta t_{max} = \alpha \left(\frac{\mu_{min}\sigma t}{8}\right)^{1/2} \Delta_{min}. \tag{32}$$

We restore the second-order scheme derived previously at other times. The transition from the fourth-order scheme to the second-order scheme takes place at a model-dependent delay time. The reason for using the adaptive algorithm is that the fourth-order scheme is more time-consuming than the second-order scheme, and more importantly, that there is no need to use the fourth-order scheme all the time. This can be seen through the following error analysis.

The accuracy of the results is controlled by the accuracy of both the spatial and temporal differences. The composite error for equations (30) and (31) can be written

$$\varepsilon = O[3\Delta^4 + (\Delta t/\mu\sigma)^2], \tag{33}$$

where, for simplicity, we assume that the medium is homogeneous and the grid spacings are the same in each Cartesian direction. The first term on the right-hand side of equation (33) results from the approximations to the spatial derivatives, the second term from the approximations to the time derivatives. Substituting equation (32) into equation (33) yields

$$\varepsilon = O[3\Delta^4 + t\alpha^2\Delta^2/(8\mu\sigma)].$$

Thus at early time the accuracy is approximately fourth-order, depending on μ and σ. As t increases, the last term gradually dominates the errors and the accuracy of the results is eventually second order.

NUMERICAL EXAMPLES

In this section we check our FDTD solution against analytical, integral equation, and spectral differential-difference solutions. The models used include (1) a vertical magnetic dipole on a homogeneous half-space, (2) a 3-D conductive body in a homogeneous or layered earth, with the resistivity contrast variable between the body and the host, (3) a 3-D conductive, magnetically permeable body in an otherwise homogeneous earth, and (4) a 3-D conductor along a vertical contact beneath a conductive overburden. The first model is the simplest, while the last one is the most complicated, aimed at showing the ability of the FDTD solution in modeling complex earth structures. The models are typically divided into 100 x 100 prisms in the horizontal directions and 50 prisms in the vertical direction, with the smallest prism 10 m on each edge. The total number of unknowns is about 3 million, requiring a minimum storage of about 12 megabytes.

Homogeneous half-space

Consider a vertical magnetic dipole on a homogeneous half-space of 100 $\Omega \cdot$ m. The FDTD responses along the positive x-axis are shown in Figure 3 at four times, ranging from 0.1 to 10 ms. The vertical and horizontal electro-motive forces (emf) correspond to the magnetic field measured with horizontal and vertical unit-moment coils, respectively. The parameter α in equations (21) and (32), which controls the time steps, is 0.1 for these computations. The FDTD responses are in good agreement with the analytical responses (Ward and Hohmann, 1988). The outward expansion of the smoke ring (Nabighian, 1979) causes the drifting of the cross-over with time. This example is important because it shows that by constraining the time steps according to equations (21) and (32), the effect of the fictitious displacement current $\gamma\partial e/\partial t$ is negligible. In this example, the maximum time step is about 4 μs, nearly 20 times larger than that given by the classic forward-difference scheme. The execution time is approximately 5.5 hours on an IBM 3090/600S computer.

To study the sensitivity of the FDTD solution to the time steps, we recomputed the responses using larger time steps [with $\alpha = 0.2$ in equations (21) and (32)]. Now the maximum time step is increased to about 8 μs. Figure 4 shows that the FDTD solution is now slightly worse than before. At that price, however, the execution time has been reduced to about 60 percent of the previous run. As a compromise between solution accuracy and computing time, we shall use $\alpha = 0.2$ in the subsequent examples.

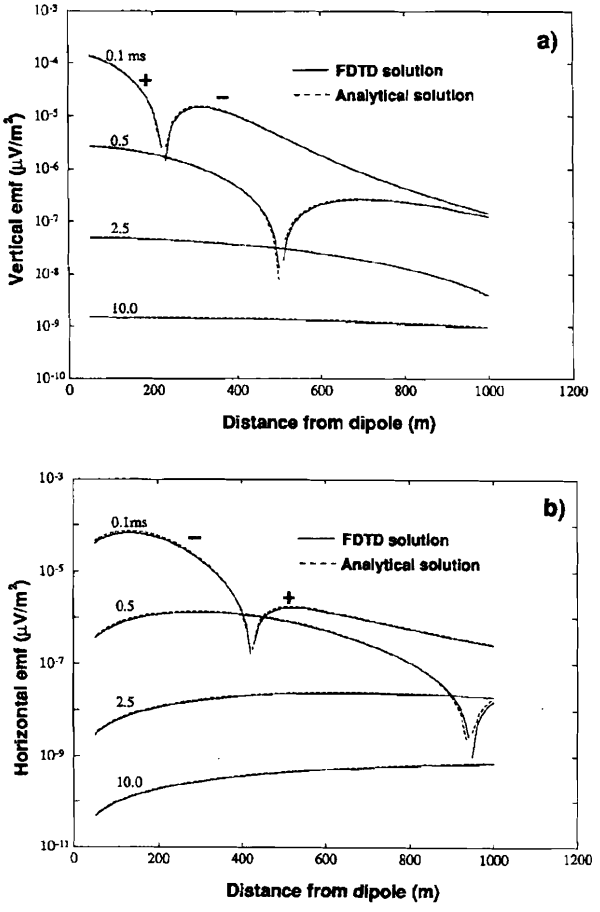

FIG. 3. Comparison of the FDTD (dashed line) and the analytical (solid line) solutions for (a) the vertical emf $(-\partial b_z/\partial t)$, and (b) the horizontal emf $(-\partial b_x/\partial t)$, due to a vertical magnetic dipole of unit moment on the surface of a 100 $\Omega \cdot$ m half-space. The symbols "+" and "-" stand for positive and negative values, respectively.

3-D body in a homogeneous half-space-low resistivity contrast

Newman et al. (1986) computed the transient response of a low-contrast 3-D model shown in Figure 5, using a frequency-domain integral-equation technique. The 0.5 Ω · m body is 100 m long, 40 m wide, 30 m in depth extent, and is 30 m deep. It is embedded in a 10 Ω · m homogeneous half-space and excited by a 100 m X 100 m loop source on the surface. Figure 5 also shows the central-loop soundings from both the integral-equation and the FDTD solution. The two solutions fall in good agreement with each other. The FDTD solution shows a slightly smaller decay rate at late times than does the integral-equation solution.

3-D body in a homogeneous half-space—intermediate resistivity contrast

As a check for a higher contrast (200:1) model, let us compare the FDTD solution to San Filipo and Hohmann's (1985) integral-equation solution for the model shown in Figure 6. Here a coincident-loop configuration is used. San Filipo and Hohmann's solution is formulated directly in the time-domain. The two solutions demonstrate an excellent agreement with each other after 1 ms. Before 1 ms, the FDTD response is slightly larger. The discrepancy is most likely caused by the different source current forms used. San Filipo and Hohmann's solution assumes a linear termination of the steady current over a time of 0.165 ms, while the FDTD solution approximates a step shut-off of the source current.

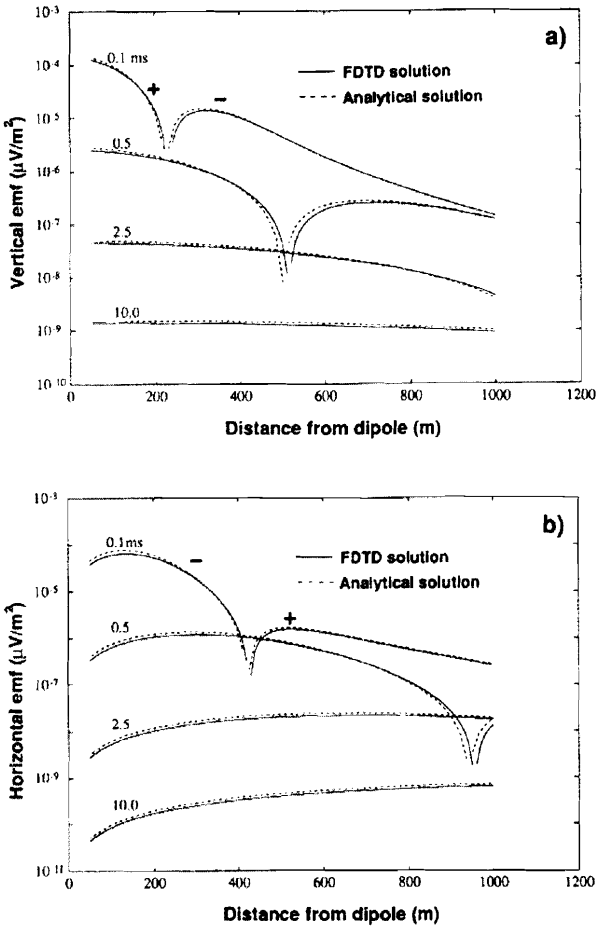

FIG. 4. Same as Figure 3, except that the time steps are doubled.

3-D body in a two-layer earth-high resistivity contrast

For the last check against an integral-equation solution, we computed a model shown in Figure 7. In this model, a 0.1 Ω m body is located in the lower layer of a two-layer earth. The body is 25 m thick, 100 m in depth extent and

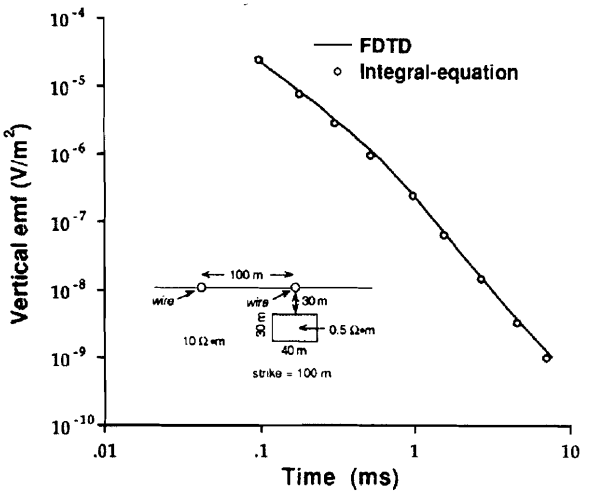

FIG. 5. Comparison of the FDTD and an integral-equation (Newman et al., 1986) solutions for a central-loop survey over a 3-D conductor. The resistivity contrast is 20.

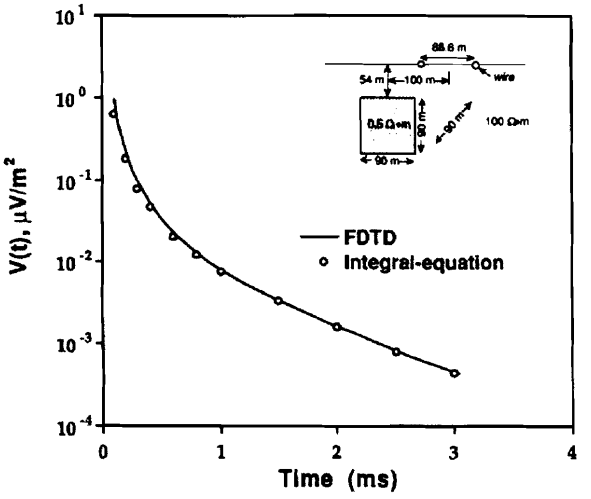

FIG. 6. Comparison of the FDTD and an integral-equation (San Filipo and Hohmann, 1985) solutions for a coincident-loop sounding over a 3-D cubic conductor in the earth. The resistivity contrast is 200.

800 m long, and is buried at a depth of 100 m. The resistivities of the upper and lower layers are, respectively, 10 Ω · m and 1000 Ω · m. Results from the FDTD solution and the integral-equation solution (Newman and Hohmann, 1988) are shown at six times ranging from 0.5 to 15 ms. Again, both solutions show good agreement, even though larger discrepancies occur to the right of the body at 3,5, and 10 ms, and to the left of the body at 15 ms.

3-D permeable body in a homogeneous half-space

Next we compare our FDTD solution to a spectral differential-difference solution (Druskin and Knizhnerman, 1988; A. Hordt, 1991, pers. comm.). The model is a 3-D body embedded in a uniform half-space (Figure 8). The body is 100 m x 100 m x 50 m and is buried at a depth of 80 m. It has a resistivity of 0.333 Ω · m and a relative magnetic permeability of 30. The half-space is of 100 Ω · m and its magnetic permeability is the same as that of free space. The resistivity and magnetic permeability contrasts of this model are 300 and 30, respectively. The large resistivity contrast is not unusual in the real world; the high magnetic permeability contrast, however, is not common. The purpose of using the unrealistic value is only for testing the algorithm. A square loop 100 m on a side is laid on the surface. The vertical emf soundings at $x = 0$ and 140 m are shown in Figure 9, and the horizontal component at $x = 140$ m is shown in Figure 10. For comparison, also shown are the responses when the body is nonpermeable. In general, the FDTD solution agrees with Druskin and Knizhnerman's solution, especially for the nonpermeable model.

At early times (before 0.2 ms) there is little difference between the permeable and nonpermeable model responses, since the body is masked by the conductive half-space. After that, the permeable model gives much higher responses than does the nonpermeable model. The late-time decay rates for the permeable model are slower than those for the nonpermeable model, because the time constant of the former is larger (Nabighian and Macnae, 1991).

3-D conductor at a vertical contact

The last model we computed is representative of a type of model that cannot be easily simulated with an integral-equation solution. The model shown in Figure 11 consists of two quarter spaces and a 3-D body overlain by a 10 Ω · m overburden. To the left of the contact is a 300 Ω · m quarter space and to the right a 100 Ω · m quarter space; along the top part of the contact is a 3-D body representing mineralization along the contact. The body is 400 m long, 50 m wide, and 200 m in depth extent, with a resistivity of 1 Ω · m.

Figure 12 shows the profile variations of the vertical emf along the positive x-axis for $t = 0.23$, 0.75, 2.4, 3.4, 5.3, and 7.8 ms. Also shown are the results computed with a spectral differential-difference method (Druskin and Knizhnerman, 1988; A. Hordt, 1991, pers. comm.). The two solutions agree overall with each other at all the times shown. At 0.23 and 0.75 ms, the responses are much like those for a layered earth (Hoversten and Morrison, 1982). At intermediate times (2.4 and 3.4 ms), drift of the cross-over to the right is slowed down due to the 3-D body and the more conductive quarter space to the right of the contact. At later times (5.3 and 7.8 ms), the cross-over passes the contact and moves rapidly to the right.

Oristaglio and Hohmann (1984) showed, for a 2-D problem, that the cross-over may move back at late times and be located above the body, which is diagnostic of the horizontal location of the body. However, the backward movement of the cross-over is not observed in this model, because the response of the 3-D body is not large enough.

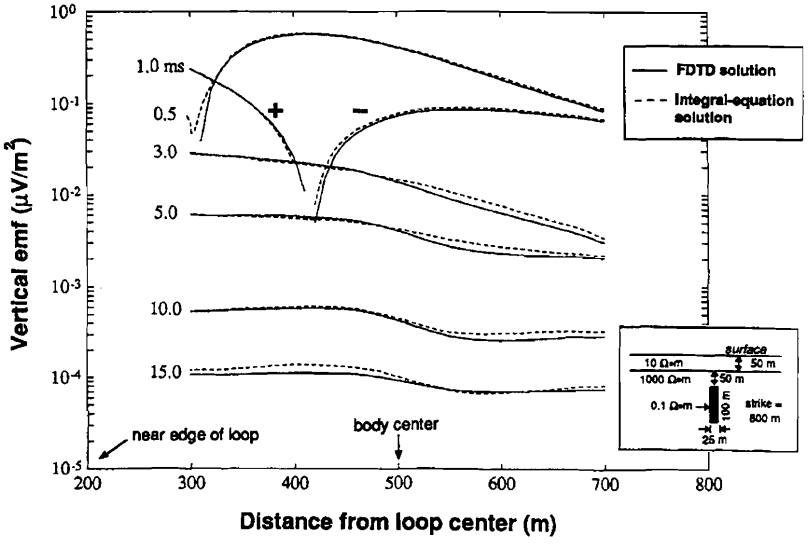

FIG. 7. Comparison of the FDTD and an integral-equation (Newman and Hohmann, 1988) solutions for a high-contrast model. A 500 m x 500 m transmitter loop is located 500 m from its center to the body center. The thickness of the body is 25 m and its strike length, depth extent, depth of burial are 800 m, 100 m, and 100 m, respectively. The symbols "+" and "-" stand for positive and negative values, respectively.

CONCLUSIONS

We have developed a finite-difference time stepping solution to the quasi-static Maxwell's equations. The solution possesses a number of appealing features. First, it can handle a complex earth model in which both conductivity and magnetic permeability vary arbitrarily in space. Second, the formulation is simple and computer implementation is easy. Third, there is no need to evaluate spatial derivatives of the physical properties, and thus the algorithm avoids the possible errors associated with it. Moreover, the solution is based on an explicit time-stepping scheme; it does not require matrix inversion. Finally, the solution provides all the electric and magnetic components throughout the earth. On the one hand, solving for all the field components appears to be a disadvantage since it doubles the computer storage requirement compared to solving for either the electric or magnetic field. It does, however, avoid many repeated operations and thus increases the numerical efficiency.

The execution time for a typical model is about 3.5 hours on an IBM 3090/600S computer to compute the field to 10 ms. The model contains 100 x 100 x 50 grid points and possesses one plane of symmetry (the x-z-plane), with the smallest grid spacing 10 m and the highest resistivity 100 $\Omega \cdot$ m.

In this paper, we have solved for the total fields. An alternative approach is to solve for the secondary fields (defined as the difference between the total field and the primary field of a background model). By solving for the secondary field, one can use a coarser mesh. As a result, computer storage and execution time are reduced. This approach has been successfully applied to a 2-D problem as reported in Adhidjaja et al. (1985). It can also be applied to a 3-D problem. The only difficulty is that computing the 3-D primary fields can be very expensive and the approach is not cost effective.

A rectangular grid has been long used in TEM modeling. Apart from its simplicity, the rectangular grid is not necessarily efficient. For example, in a graded grid, the prisms near the grid boundaries may be unnecessarily small along some Cartesian directions, resulting in an oversampling of the field. To overcome the problem, one can use a subgridding technique (Zivanovic et al., 1991). With this technique, the model is first discretized into large, approximately equidimensional prisms. Then those prisms experiencing sharp field variations are further discretized into smaller prisms. The process is repeated until all the prisms are small enough compared to the spatial wavelengths of the field. The result-

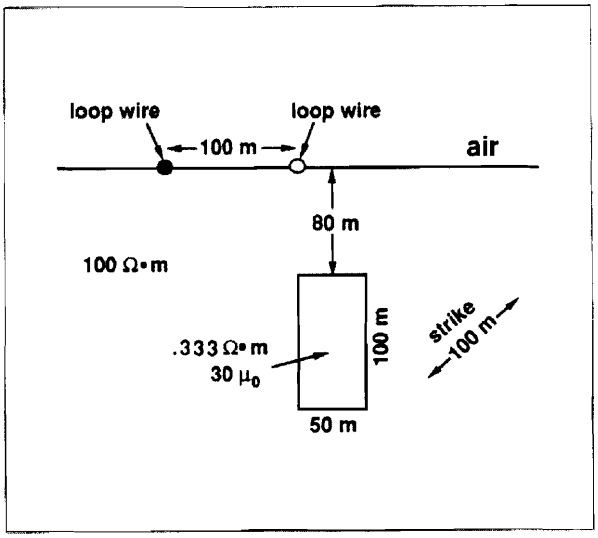

FIG. 8. A 3-D model used for comparing the FDTD solution with a spectral differential-difference method. The resistivity and magnetic permeability contrasts between the body and the half-space are, respectively, 300 and 30.

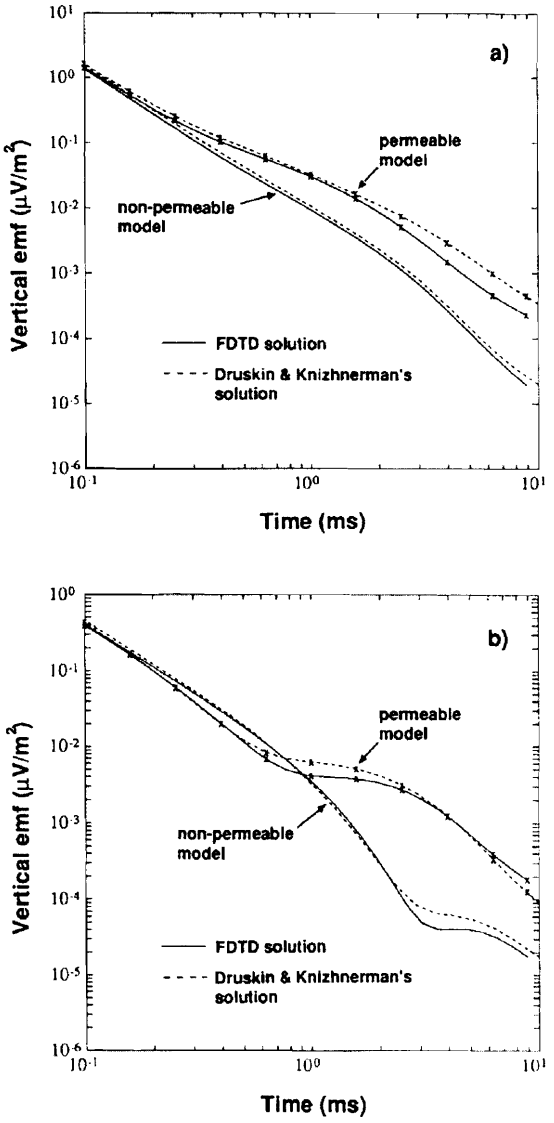

FIG. 9. Comparison of the FDTD and Druskin and Knizhnerman's (1988) spectral differential-difference solutions for the vertical emf soundings for the model shown in Figure 8. (a) x = 0 m, (b) x = 140 m.

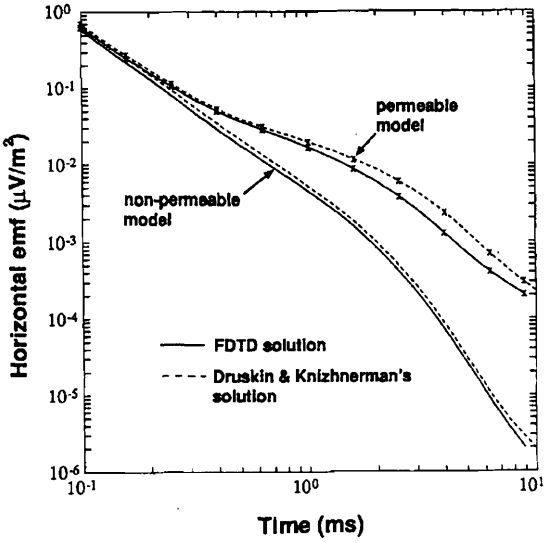

FIG. 10. Same as Figure 9, except for the horizontal component at x = 140 m.

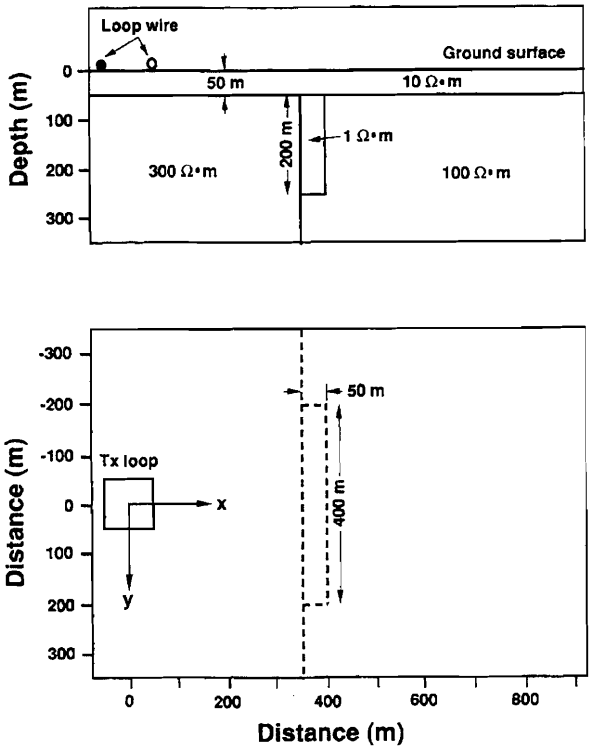

FIG. 11. A vertical contact model. (a) Section view, (b) Plan view. The maximum resistivity contrast is 300. A 100 by 100 m loop is laid to the left of the contact on the surface.

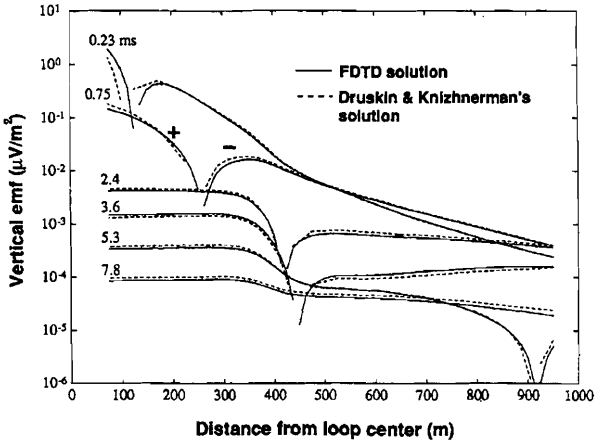

FIG. 12. Comparison of the FDTD and Druskin and Knizhnerman's (1988) spectral differential-difference solutions for the contact model shown in Figure 11. The symbols "+" and "-" stand for positive and negative values, respectively.

ing grid usually contains fewer grid nodes than does the conventional rectangular grid. Such a grid, however, can be quite irregular. Numerical interpolation is needed to compute the field values at the irregular grid nodes.

ACKNOWLEDGMENTS

We would like to thank Drs. L. P. Beard, Y. Luo, M. L. Oristaglio, B. R. Spies, and A. C. Tripp for their invaluable suggestions and comments, A. Hordt for providing the model results using a spectral differential-difference method. T. Wang is grateful to Dr. Y. Luo for suggesting Yee's staggered-grid technique. He is indebted to Dr. W. C. Chew, Dr. V. Druskin, and an anonymous reviewer for their thoughtful review of the original manuscript, and to the Associate Editor, Dr. M. L. Oristaglio, for helping improve the manuscript. Funding for this study was provided through the University of Utah Consortium for Electromagnetic Modeling and Inversion (CEMI), which is supported by BHP-Utah Minerals, B. P. Research, CRA Exploration FMC Gold, Geothermal Energy Research and Development, Kennecott Exploration, Mobil Research and Development, Noranda, Schlumberger-Doll Research, Shell Exploratie en Produktie Laboratorium, and Unocal. A grant of computer time from the Utah Supercomputing Institute, which is funded by the State of Utah and the IBM Corporation, is gratefully acknowledged.

REFERENCES

Adhidjaja, J. I., and Hohmann, G. W., 1989, A finite-difference algorithm for the transient electromagnetic response of a three-dimensional body: Geophys. J. Int., 98, 233-242.

Adhidjaja, J. I., and Hohmann, G. W., and Oristaglio, M. L., 1985, Two-dimensional transient electromagnetic responses: Geophysics, 50, 2849-2861.

Alford, R. M., Kelly, K. R., and Boore, D. M., 1974, Accuracy of finite-difference modeling of the acoustic wave equation: Geophysics, 39, 834-842.

Bergeal, J. M., 1982, The test of an explicit scheme in modeling

/transient electromagnetic fields in mining geophysics: MS thesis, Yale University.
Best, M. E., Duncan, P., Jacobs, F. J., and Scheen, W. L., 1985, Numerical modeling of the electromagnetic response of three-dimensional conductors in a layered earth: Geophysics, 50, 665-676.
Birtwistle, G. M., 1968, The explicit solution of the equation of heat conduction: Comput. J., 11, 317-323.
Chew, W. C., 1990, Waves and fields in inhomogeneous media: Van Nostrand Reinhold, New York.
Du Fort, E. C., and Frankel, S. P., 1953, Stability conditions in the numerical treatment of parabolic differential equations: Math. tables and other aids to comput. (former title of Math. Comput.), 7, 135-152.
Druskin, V. L., and Knizhnerman, L. A., 1988, Spectral differential-difference method for numeric solution of three-dimensional nonstationary problems of electric prospecting: Izvestiya: Earth Phys., 24, 641-648.
Goldman, M. M., and Stoyer, C. H., 1983, Finite-difference calculations of the transient field of an axially symmetric earth for vertical magnetic dipole excitation: Geophysics, 48, 953-963.
Grant, F. S., and West, G. F., 1965, Interpretation theory in applied geophysics: McGraw-Hill Book Co.
Greenfield, R. J., and Wu, S. T., 1991, Electromagnetic wave propagation in disrupted coal seams: Geophysics, 56, 1571-1577.
Hohmann, G. W., 1988, Numerical modeling for electromagnetic methods of geophysics, in Nabighian, M. N., Ed., Electromagnetic methods in applied geophysics, Investigations in Geophysics 3, Vol. 1: Soc. Expl. Geophys.
Holland, R., Simpson, L., and Kunz, K. S., 1980, Finite-difference analysis of EMP coupling to lossy dielectric structures: IEEE Trans Electromag. Compat., EMC-22, 203-209.
Hoversten, G. M., and Morrison, H. F., 1982, Transient field of a current loop source above a layered earth: Geophysics, 47, 1068-1077.
Kelly, K. R., Ward, R. W., Treitel, S., and Alford, R. M., 1976, Synthetic seismograms: A finite-difference approach: Geophysics, 41, 2-27.
Luo, Y., 1989, Solving 2-D and 2.5-D finite-difference electromagnetic field modeling: Ann. Rep., Univ. of Utah Tomography Development Project.
Macnae, J. C., 1984, Survey design for multicomponent electromagnetic systems: Geophysics, 49, 265-273.
Madden, T. R., and Mackie, R. L., 1989, Three-dimensional magnetotelluric modeling and inversion: Proc. IEEE, 77, 318-333.
Mitchel, A. R., and Griffiths, D. F., 1980, The finite-difference method in partial differential equations: John Wiley & Sons, Inc.
Moghaddam, M., Yannakakis, E., Chew, W. C., and Randall, C., 1991, Modeling of the subsurface interface radar: J. Electromagn. Waves Appl., 5, 17-39.
Mufti, I. R., 1990, Large-scale, three-dimensional seismic models and their interpretive significance: Geophysics, 55, 1166-1 182.
Nabighian, M. N., 1972, The analytic signal of two-dimensional magnetic bodies with polygonal cross-section: Its properties and use for automated interpretation: Geophysics, 37, 507-517.
- 1979, Quasi-static transient response of a conducting half-space: An approximate representation: Geophysics, 44, 1700-1705.
- 1984, Toward a three-dimensional automatic interpretation of potential field data via generalized Hilbert transforms: Fundamental relations: Geophysics, 49, 780-786.
Nabighian, M. N., and Macnae, J. C., 1991, Time-domain electromagnetic prospecting methods: *in* Nabighian, M. N., Ed., Electromagnetic methods in applied geophysics, Investigations in Geophysics 3, vol. 2, Part A: Soc. Expl. Geophys.
Nekut, A. G., and Spies, B. R., 1989, Petroleum exploration using controlled-source electromagnetic methods: Proc. IEEE, 77, 338-362.
Newman, G. A., and Hohmann, G. W., 1988, Transient electromagnetic responses of high-contrast prisms in a layered earth: Geophysics, 53, 691-706.
Newman, G. A., and Hohmann, G. W., and Anderson, W. L., 1986, Transient electromagnetic response of a three-dimensional body in a layered earth: Geophysics, 51, 1608-1627.
Oristaglio, M. L., and Hohmann, G. W., 1984, Diffusion of electromagnetic fields into a two-dimensional earth: A finite-difference approach: Geophysics, 49, 870-894.
San Filipo, W. A., and Hohmann, G. W., 1985, Integral equation solution for the transient electromagnetic response of a three-dimensional body in a conductive half-space: Geophysics, 50, 798-809.
Stakgold, I., 1968, Boundary value problems of mathematical physics, vol. II: John Wiley & Sons, Inc.
Taflove, A., 1980, Application of the finite-difference time-domain method to sinusoidal steady-state electromagnetic-penetration problems: IEEE Trans Electromag. Compat., EMC-22, 191-202.
Taflove, A., and Brodwin, M. E., 1975, Numerical solution of steady-state electromagnetic scattering problems using the time-dependent Maxwell equations: IEEE Tran. Microwave Theory Tech., MTT-23, 623-630.
Virieux, J., 1984, SH-wave propagation in heterogeneous media: Velocity-stress finite-difference method: Geophysics, 49, 1933-1957.
——— 1986, *P-SV* wave propagation in heterogeneous media: Velocity-stress finite-difference method: Geophysics, 51, 889-901.
Visscher, P. B., 1989, Discrete formulation of Maxwell equations: Computers in Physics, 3, 42-45.
Ward, S. H., and Hohmann, G. W., 1988, Electromagnetic theory for geophysical applications, *in* Nabighian, M. N., Ed., Electromagnetic methods in applied geophysics, Investigations in Geophysics 3, vol. 1: Soc. Expl. Geophys.
Yee, K. S., 1966, Numerical solution of initial boundary problems involving Maxwell's equations in isotropic media: IEEE Trans. Ant. Prop., AP-14, 302-309.
Zivanovic, S. S., Yee, K. S., and Mei, K. K., 1991, A subgridding method for the time-domain finite-difference method to solve Maxwell's equations: IEEE Trans. Microwave Theory and Tech., MTT-39, 471-479.

APPENDIX

THE FOURTH-ORDER, FINITE-DIFFERENCE APPROXIMATION

Define the discrete values of a function f at nodes i as f_i. The grid spacing between nodes i and $i + 1$ is Δx_i. The fourth-order, finite-difference approximation to df/dx at node $i + 1/2$ can be written

$$\left(\frac{df}{dx}\right)_{i+1/2} \approx c_{-1}f_{i-1} + c_0 f_i + c_1 f_{i-1} + c_2 f_{i+2}, \quad \text{(A-1)}$$

where c's are the coefficients to be determined. Using a Taylor expansion of f_i 's at $x = x_i + \Delta x_i/2$ and equating the coefficients of both sides associated with the derivatives of the same order, we have the following system of equations

$$\begin{bmatrix} 1 & 1 & 1 & 1 \\ -\ell_{-1} & -\ell_0 & \ell_1 & \ell_2 \\ \ell_{-1}^2 & \ell_0^2 & \ell_1^2 & \ell_2^2 \\ -\ell_{-1}^3 & -\ell_0^3 & \ell_1^3 & \ell_2^3 \end{bmatrix} \begin{bmatrix} c_{-1} \\ c_0 \\ c_1 \\ c_2 \end{bmatrix} = \begin{bmatrix} 0 \\ 1 \\ 0 \\ 0 \end{bmatrix}. \quad \text{(A-2)}$$

Here,

$$\ell_{-1} = \Delta x_{i-1} + \Delta x_i/2,$$

$$\ell_0 = \Delta x_i/2,$$

$$\ell_1 = \Delta x_i/2,$$

$$\ell_2 = \Delta x_i/2 + \Delta x_{i+1}.$$

The system of equations (A-2) can be easily solved for c's.